

Regular article

A theoretical study of the $\text{H}_2\text{SO}_4 + \text{H}_2\text{O} \rightarrow \text{HSO}_4^- + \text{H}_3\text{O}^+$ reaction at the surface of aqueous aerosols

Roberto Bianco¹, James T. Hynes^{1,2}

¹Department of Chemistry and Biochemistry, University of Colorado, Boulder, CO 80309-0215, USA

²Département de Chimie, CNRS UMR 8640 PASTEUR, Ecole Normale Supérieure, 24 rue Lhomond, Paris 75231, France

Received: 12 March 2003 / Accepted: 30 April 2003 / Published online: 30 January 2004
© Springer-Verlag 2004

Abstract. The surface region of sulfate aerosols (supercooled aqueous concentrated sulfuric acid solutions) is the likely site of a number of important heterogeneous reactions in various locations in the atmosphere, but the surface region ionic composition is not known. As a first step in exploring this issue, the first acid ionization reaction for sulfuric acid, $\text{H}_2\text{SO}_4 + \text{H}_2\text{O} \rightarrow \text{HSO}_4^- + \text{H}_3\text{O}^+$, is studied via electronic structure calculations at the Hartree–Fock level on an H_2SO_4 molecule embedded in the surface region of a cluster containing 33 water molecules. An initial H_2SO_4 configuration is selected which could produce H_3O^+ readily available for heterogeneous reactions, but which involves reduced solvation and is consistent with no dangling OH bonds for H_2SO_4 . It is found that at 0 K and with zero-point energy included, the proton transfer is endothermic by 3.4 kcal/mol. This result is discussed in the context of reactions on sulfate aerosol surfaces and, further, more complex calculations.

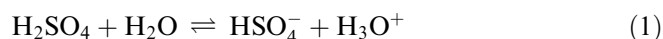
Keywords: Sulfate aerosols – Heterogeneous proton transfer

1 Introduction

Most attention concerning atmospheric ozone depletion has concentrated on the Antarctic stratosphere and the “ozone hole”, where heterogeneous chemistry involving chlorine-containing species, like HCl and ClONO₂, occurs on ice and related aerosols[1]. There is, however, important ozone depletion occurring in other atmospheric locations. One important example is the midlatitude stratosphere, where the aerosols providing heterogeneous reaction sites are instead sulfate aerosols, highly concen-

trated supercooled aqueous solutions of ~ 60–80% in weight (~ 22–42 mol%) of sulfuric acid [2–4], with a corresponding $\text{H}_2\text{SO}_4/\text{H}_2\text{O}$ molecular ratio ~ 0.25–1. In this region, perhaps the most important heterogeneous reaction is the net hydrolysis of dinitrogen pentoxide $\text{N}_2\text{O}_5 + \text{H}_2\text{O} \rightarrow 2\text{HNO}_3$ which plays a key role in stratospheric ozone depletion [2–7]. There are additional heterogeneous reactions of importance as well [4]. Further, sulfate aerosols are also found in the Arctic boundary layer, and heterogeneous chemistry on/in them is implicated in ozone depletion there[8, 9]. Finally, it has recently been suggested [1] that sulfate aerosols, rather than ice or related aerosols, may actually provide the most important reaction sites in the Antarctic stratosphere. Since a number of such heterogeneous reactions will occur in the surface region of sulfate aerosols, it is important to have information on the character of those surfaces.

The bulk ionic composition of sulfate aerosols appears to be well described by detailed thermodynamic models that have been developed [10]. Thus, at given temperature and relative humidity, the ratio $\text{H}_2\text{SO}_4/\text{HSO}_4^-/\text{SO}_4^{2-}/\text{H}_3\text{O}^+/\text{H}_2\text{O}$ can be regarded as known in the bulk of the aerosol for a given weight percentage of sulfuric acid. Since, however, the surface can be regarded as in some sense “less polar” than the bulk, the question can be raised as to whether the ionic composition would be the same in the surface region as it is in the bulk. Thus, for example, for a bulk ionic composition consisting exclusively of $\text{HSO}_4^-/\text{H}_3\text{O}^+/\text{H}_2\text{O}$, could there be back proton transfer in the surface region to produce some molecular H_2SO_4 from the bisulfate ion HSO_4^- and the hydronium ion H_3O^+ ? This is the reverse reaction for the sulfuric acid first acid dissociation:



While a complete investigation of the $\text{H}_2\text{SO}_4/\text{HSO}_4^-/\text{H}_3\text{O}^+$ surface issue would involve the examination of the reaction Eq. (1) in the surface region in the presence of the various ions in the bulk below that region, an important initial step on the road to answering the question is to examine the first acid ionization step for H_2SO_4 in the surface region of a model for supercooled water.

Contribution to the Jacopo Tomasi Honorary Issue

Correspondence to: R. Bianco
e-mail: roberto.bianco@colorado.edu

This issue for the surface ionic composition involving molecular H_2SO_4 and/or HSO_4^- and its hydronium counterion is important for the possibility of having protons readily available for the acid catalysis of surface reactions, either directly or via a short sequence of proton transfers to surface water molecules. (Closely related questions and issues arise when there is significant concentration of sulfate ions SO_4^{2-} in the bulk.). While the molecular morphology of the surface of sulfate aerosols has been the subject of important studies, both on the experimental [11–17] and theoretical [18, 19] sides, the ionic composition issue in the H_2SO_4 weight percentage appropriate for atmospheric sulfate aerosols remains poorly understood. In this paper we examine the first acid ionization reaction (Eq. 1) for an H_2SO_4 molecule embedded at the surface of a model water lattice.

We should note that clusters containing both H_2SO_4 and H_2O in various amounts and ratios have been studied both experimentally [11, 20] and theoretically [21–24]; however, as we have stressed elsewhere [25], the absence in small clusters of the natural constraints arising at an aqueous surface make these model systems questionable for the aerosol situation, even when they involve high-level electronic structure calculations. Large-cluster studies involving classical rather than quantum interactions also exist [26]. Other cluster studies have focussed on the issue of production of H_2SO_4 from SO_3 and have found the $\text{HSO}_4^- \cdot \text{H}_3\text{O}^+$ contact ion pair as a by-product [23, 24].

The outline of this paper is as follows. We discuss the model reaction system in Sec. 2. We detail the computational strategy in Sec. 3 and present the results in Sec. 4. We offer concluding remarks in Sec. 5.

2 Model reaction system

Our focus is on the possibility of the first acid ionization of H_2SO_4 , Eq. 1. In solution, the second ionization step to produce the sulfate ion (not examined here) is much less likely than the first ionization [27] and, at the water surface, the solvation conditions are significantly less favorable for the ionization than in solution: one could loosely say that half the solvation of, for example, the HSO_4^- ion is missing at the surface compared to the bulk. In this sense, our model reaction system represents a limiting case where the dissociation of H_2SO_4 is difficult owing to the lack of solvation, as discussed further later. If H_2SO_4 were to dissociate in these disadvantageous conditions, one could say with confidence that the $\text{H}_3\text{O}^+ \cdot \text{HSO}_4^-$ ion pair is present at the surface of sulfate aerosols (at least of the diluted ones), thus portraying a heightened capability of the surface to catalyze heterogeneous reactions.

We consider the $\text{H}_2\text{SO}_4 \cdot (\text{H}_2\text{O})_6 \cdot \text{W}_{27}$ model reaction system displayed in Fig. 1, where the $\text{H}_2\text{SO}_4 \cdot (\text{H}_2\text{O})_6$ core reaction system (CRS) is treated quantum chemically, whereas the W_{27} embedding water (W) lattice is treated classically. In the following, we describe the motivation for the H_2SO_4 placement in Fig. 1 and the choice of the CRS.

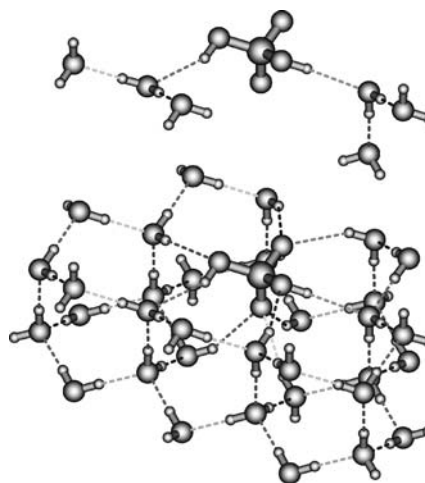
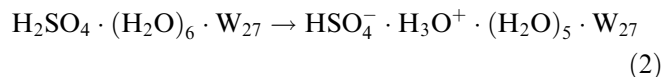


Fig. 1. *Top:* $\text{H}_2\text{SO}_4 \cdot (\text{H}_2\text{O})_6$ core reaction system (CRS). *Bottom:* $\text{H}_2\text{SO}_4 \cdot (\text{H}_2\text{O})_6$ CRS embedded in the W_{27} effective fragment potentials water lattice—this larger cluster was used in the calculations

An initial H_2SO_4 configuration is selected which could produce H_3O^+ readily available for heterogeneous reactions, but which involves reduced solvation and is consistent with no dangling OH bonds for H_2SO_4 . In the particular placement selected for the H_2SO_4 moiety, each of its potentially proton-donating hydroxyl groups is located in the top layer of the surface, and is hydrogen-bonded to a water molecule. An alternative placement, with one dangling OH group of the H_2SO_4 , was discarded on the ground that such an acidic proton would most likely be found hydrogen-bonded to an O lone pair of surface water, instead of remaining uncoordinated, a common feature for the much less acidic protons of an H_2O molecule at a pure water surface [28]. The selected configuration can be contrasted with two further ones in which one or both of the hydroxyls would be oriented toward the bulk of the lattice. Then, owing to the increased solvation of the bulk OH(s), the likelihood of dissociation would be enhanced.

Each sulfuric acid proton is hydrogen-bonded to a water molecule, also described quantum-chemically, since it can accept the proton and become a hydronium ion: In turn, this water has its two protons hydrogen-bonded to two other quantum waters, thus providing the tricoordination required [29, 30] for the ensuing hydronium ion. Later, we focus on the acid dissociation



to assess if the electronic polarization of the sulfate group and the relaxation of the lattice can stabilize the ensuing surface ions in conditions of limited solvation that we have just described.

3 Computational methodology

We used the quantum chemistry suite of programs GAMESS [37]. For the quantum portion of the model reaction system, we used the

Stevens–Bash–Krauss (SBK)[32] effective core potential basis set, complemented by polarization (S exponent 0.65 [33], O exponent 0.8 [34]) and diffuse (S exponent 0.0405 [35], O exponent 0.0845 [36]) functions on the heavy atoms, i.e. SBK + (d). The classical water molecules are represented by effective fragment potentials [37]. The calculations were performed at the Hartree–Fock level as follows.

First, we partially optimized and embedded the H_2SO_4 moiety in the orientation shown in Fig. 1 into the basal plane face of a model hexagonal ice lattice assembled via replication of its unit cell [38]. Initially, the ice lattice contained only the oxygen atoms. The oxygens overlapping (in a Van der Waals fashion) the H_2SO_4 atoms were discarded; then the hydrogens of the oxygens in the first solvation shell, i.e. directly coordinated to H_2SO_4 , were assigned, with the constraints that all waters be hydrogen-bonded both to the solute atoms and among themselves, and with the further requirement that the sum of the dipole moments of the first solvation shell waters and H_2SO_4 (the latter previously calculated for the isolated species) falls below a given low threshold. The assignment of hydrogens was made by screening numerous configurations obtained via permutation of the six allowed orientations of the dipole moment of each water. The hydrogens of the outer solvation shells were assigned shell by shell, starting from the second, maintaining the constraint that the resulting lattice be fully hydrogen-bonded. No dipole moment partial minimization was sought for the outer shells. After all the hydrogens had been assigned, the two water trimers coordinated to the two H_2SO_4 acidic protons were identified and represented quantum chemically, as explained in Sect. 2. Finally, the model reaction system was reduced in size by manually selecting (1) the waters in the first solvation shell of the $\text{H}_2\text{SO}_4\cdot(\text{H}_2\text{O})_6$ moiety, (2) the waters stabilizing the first solvation shell, and (3) the external waters in the second monolayer to prevent the waters in first monolayer close to the edge from migrating from their initial positions. The size of the lattice reflects the following requirements: (1) that the CRS be fully solvated, (2) that the CRS plus the first solvation shell be kept in place by a number of extra waters to prevent the collapse of the whole cluster along the reaction path, and (3) that the number of extra waters be minimal to limit the computational cost. The full optimization of the model reaction system so assembled yielded the initial reactant complex (RC) used for the transition-state (TS) search.

Starting from the RC, we located the TS ($\bar{\nu} = 530i \text{ cm}^{-1}$) by reducing in a stepwise fashion the $\text{H}_2\text{O}\cdots\text{HOSO}_3\text{H}$ distance between one of the acidic protons and the oxygen of its hydrogen-bonded water molecule to force the formation of a H_3O^+ hydronium ion. For each fixed $\text{H}_2\text{O}\cdots\text{HOSO}_3\text{H}$ distance, all the other internal coordinates of the cluster were optimized. The optimized structure of both the RC and the product complex (PC) were then obtained via calculation of the intrinsic reaction coordinate path [39]. The stationary points were confirmed by a Hessian calculation.

4 Results

The RC, TS and PC are displayed in Fig. 2, whereas their corresponding CRSs, referred to in the ensuing discussion, are displayed in Fig. 3.

We highlight some of the key features of the mechanism at the RC, TS, and PC in Table 1. In particular, we report all the S–O and SO–H bond lengths and the average hydrogen-bond distances between the hydrogens of the solvating waters and the sulfate oxygens. The labeling in the table, referred to Figs. 2 and 3, has O_2 connected to the dissociating proton H_6 , O_3 connected to the other proton H_7 , O_4 double-bonded to S_1 in the top layer, and O_5 pointing down toward the bulk. All the S–O bond lengths except $\text{S}_1\text{--O}_2$ increase in going from the RC to the PC. This corresponds to a change in the dipole moment of the sulfate group upon formation of

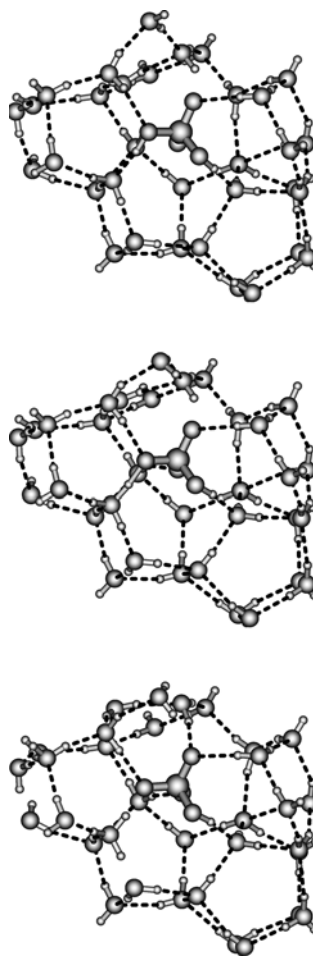


Fig. 2. From top: reactant complex (RC), transition state (TS), and product complex (PC)

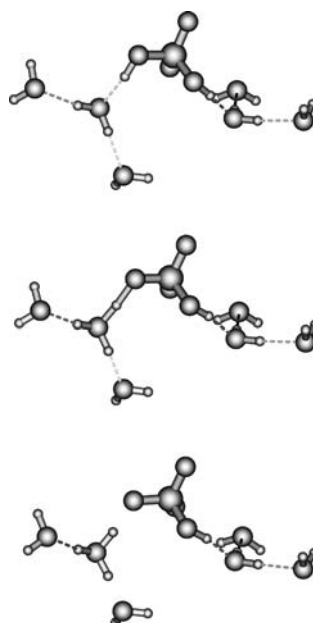


Fig. 3. From top: RC, TS, and PC CRSs

Table 1. Structure and hydrogen bonding of $\text{H}_2\text{SO}_4/\text{HSO}_4^-$ along the reaction path. O_5 is the oxygen pointing away from the viewer in Figs. 2 and 3. $\text{HOH}\cdots\text{OS}$ is the average length of the hydrogen bonds of the solvating waters to the sulfate oxygen. The number of

hydrogen bonds is that between solvating waters and sulfate oxygens. Bond lengths in angstrom. Reactant complex (RC), transition state (TS), and product complex (PC)

	$\text{S}_1\text{-O}_2$	$\text{S}_1\text{-O}_3$	$\text{S}_1\text{-O}_4$	$\text{S}_1\text{-O}_5$	$\text{S}_1\text{O}_2\text{-H}_6$	$\text{S}_1\text{O}_3\text{-H}_7$	$\text{HOH}\cdots\text{OS}$	Number of hydrogen bonds
RC	1.544	1.538	1.431	1.430	1.003	1.005	2.217	4
TS	1.496	1.554	1.442	1.442	1.273	0.992	2.216	5
PC	1.479	1.557	1.449	1.446	1.467	0.991	2.064	5

Table 2. Charge distributions of $\text{H}_2\text{O}\cdot\text{H}_2\text{SO}_4 / \text{H}_3\text{O}^+\cdot\text{HSO}_4^-$ along the reaction path. Löwdin charges in units of electronic charge. H_6 is the proton transferring to O_8

	$q(\text{S}_1)$	$q(\text{O}_2)$	$q(\text{O}_3)$	$q(\text{O}_4)$	$q(\text{O}_5)$	$q(\text{H}_6)$	$q(\text{H}_7)$	$q(\text{O}_8)$	$q(\text{H}_9)$	$q(\text{H}_{10})$
RC	1.88	-0.75	-0.73	-0.78	-0.77	0.50	0.50	-0.91	0.47	0.46
TS	1.87	-0.86	-0.74	-0.82	-0.82	0.53	0.49	-0.81	0.49	0.48
PC	1.87	-0.89	-0.74	-0.85	-0.84	0.51	0.49	-0.77	0.51	0.49

Table 3. Energetics along the reaction path. E is the absolute energy in hartrees. ΔE is the relative energy at 0 K without zero-point energy (ZPE) in kcal/mol referred to RC. ZPE is in kcal/mol. (The RC Hessian calculation showed a single imaginary frequency of $50i\text{ cm}^{-1}$ discarded from the RC ZPE calculation.) $\Delta E(\text{ZPE}) = [E(\text{A}) - E(\text{B})] + [\text{ZPE}_\text{A} - \text{ZPE}_\text{B}]$, relative energy at 0 K including ZPE in kcal/mol. 1 hartree = 627.51 kcal/mol

	E	ΔE	ZPE	$\Delta E(\text{ZPE})$
RC	-175.413385	0.0	212.3	0.0
TS	-175.408292	3.2	210.7	1.5
PC	-175.408987	2.8	212.9	3.4

the $\text{HSO}_4^-\cdot\text{H}_3\text{O}^+$ contact ion pair. The $\text{O}_3\text{-H}_7$ distance decreases slightly, as expected.

In the cluster, O_4 has two hydrogen bonds with the solvating waters in the RC, which increase to three in the TS and PC, both O_2 and O_5 have one hydrogen bond, whereas O_3 has none. Therefore acid dissociation leads to an increase of hydrogen-bonded waters and a decrease in hydrogen-bonded distances, with the top-layer O_4 appearing the most affected. O_5 and O_3 , initially set up by the embedding algorithm with three and one hydrogen bonds, respectively, with the lattice solvating waters (Fig. 1), appear to have a reduced interaction with the latter in the optimized RC. This is counter to the intuitive notion that each oxygen in the sulfate group could support at least two hydrogen bonds. It is possible, however, that the sulfate-water interaction suffers somewhat from a lack of lattice constraints and the consequent increased rotational degrees of freedom of the solvating waters, resulting in the apparent reduced solvation. This would indicate that the cluster of embedding waters should be augmented in size to verify this feature.

The charge distribution of the $\text{H}_2\text{SO}_4\cdot\text{H}_2\text{O}$ moiety along the reaction path is reported in Table 2. The charges for S, O_3 , and all the hydrogens are essentially constant. The negative charges on the other sulfate oxygens (O_2 , O_4 , and O_5) increase (in modulo) by an average of $0.11e$, consistent with the stronger interaction with the solvating

waters. The charge on the oxygen of the proton-accepting water (O_8) becomes more positive by $0.14e$. In the product complex, $q(\text{H}_3\text{O}^+) = 0.74e$ and $q(\text{HSO}_4^-) = -0.96e$, implying charge transfer from O_8 to the waters and the HSO_4^- coordinated to the hydronium ion.

Finally, for the reaction energy at 0 K associated with the first acid ionization, we find (Table 3) $\Delta E(\text{ZPE}) = 3.4\text{ kcal mol}^{-1}$. The key point of these results is that the H_2SO_4 acid dissociation in the selected configuration is endothermic. In addition, the TS energy without ZPE is only $\sim 0.4\text{ kcal mol}^{-1}$ higher than the PC energy. The inclusion of ZPE reduces the total energy of that “TS” to a value below that of the PC, suggesting a monotonic rise of the total energy between reactants and products. While Table 3 indicates that there are many contributing sources for the ZPE, it is useful to note that our estimates of the stretch frequencies for the transferring H for the RC, TS, and PC are 3142 , $530i$, and 2455 cm^{-1} , respectively, with the unstable TS motion found to be nearly exclusively the H motion between the oxygen atoms of the donor H_2SO_4 and the acceptor H_2O . Thus, in a simple collinear image (ignoring $\text{O}\cdots\text{H}\text{-O}$ bends), the transverse coordinate involving H at the TS is nearly a symmetric stretch in which the H is stationary, so that there is no high frequency H motion contributing to the ZPE at the TS, while there is such a contribution at, for example, the PC. This differential ZPE effect will tend to remove any barrier at the TS. This same general conclusion would also follow from an alternative view in which the proton is quantized [40, 41].

5 Concluding remarks

The present finding that the first acid ionization of sulfuric acid in the selected configuration at an aqueous surface is endothermic might be regarded as surprising, given previous theoretical work indicates that this ionization should proceed in small water clusters (four waters) [42]. However, as we have noted here and elsewhere [25], water rearrangements in small clusters

can occur without the constraints imposed by a water network, and cluster results need not be at all applicable for surface conditions. It is relevant to note that although H_2SO_4 in aqueous solution is generally regarded as a strong acid in its first acid ionization, the equilibrium constant for this dissociation is variously estimated as only 10^2 – 10^3 , values which are some 4–5 orders of magnitude smaller than estimates for HCl [27] (which is also predicted [43] to ionize in a cluster of four water molecules). Such estimates suggest that the sulfuric acid ionization is a reasonably delicate issue, and further studies (see later) will definitely be necessary before one could confidently conclude that ionization does not occur at the surface and thus that protons are not available from this source for acid catalysis of heterogeneous surface reactions. (We note, however, that proton transfer from molecular H_2SO_4 even in the configuration studied here might still be induced by further coordination with an adsorbed reactant molecule such as N_2O_5 .)

We can suggest several extensions of the present calculations. First, as noted in Sec. 2, alternative positioning of the H_2SO_4 molecule at the surface such that one OH group penetrates deeper into the system could increase solvation of the ionic products and thus promote acid ionization. Second, although there is considerable solvation of, for example, HSO_4^- in the endothermic product (see Fig. 2), additional water molecules located above the acid might provide sufficient solvation to make the reaction exothermic. The presence of such extra-lattice waters, to be expected under stratospheric conditions [30, 41, 44], has already been shown to be necessary for, for example, HBr ionization atop an ice surface [25]. Finally, the influence of the ions present in the bulk not far from the surface region may have an influence; the general effect of the electric field due to those ions should be to further stabilize the $\text{HSO}_4^- \cdot \text{H}_3\text{O}^+$ ion pair. Whether all or any of these aspects will be sufficient for the first ionization to occur such that acid catalysis is facilitated for heterogeneous surface reactions remains to be seen.

All of our discussion has focussed on the first acid ionization of H_2SO_4 . For some atmospheric conditions, the ionic composition of the bulk is characterized by extensive sulfate ion concentration as a result of the second acid ionization [10]. For these situations, a similar theoretical study of the second, and weaker, sulfuric acid ionization, $\text{HSO}_4^- + \text{H}_2\text{O} \rightleftharpoons \text{SO}_4^{2-} + \text{H}_3\text{O}^+$, will be needed.

All the aspects mentioned in the preceding two paragraphs are currently under investigation. Further, we hope to report on several heterogeneous reactions on model sulfate aerosol surfaces in the near future, including the N_2O_5 hydrolysis mentioned in Sec. 1 and the key Antarctic stratosphere reaction $\text{HCl} + \text{ClONO}_2 \rightarrow \text{Cl}_2 + \text{HNO}_3$ [1, 45, 46].

Acknowledgements. We take this opportunity to express our appreciation of Jacopo Tomasi as a scientist and as a friend. This work was supported in part by NSF grant ATM-0000542 and the CNRS. This research was performed in part using the Molecular Science Computing Facility in the William R. Wiley Environmental

Molecular Sciences Laboratory, a national scientific user facility sponsored by the U.S. Department of Energy's Office of Biological and Environmental Research and located at the Pacific Northwest National Laboratory. Pacific Northwest is operated for the Department of Energy by Battelle.

References

- Solomon S (1999) *Rev Geophysics* 37: 275
- Kolb CE, Worsnop DR, Zahniser MS, Davidovits P, Keyser LF, Leu M-T, Molina MJ, Hanson DR, Ravishankara AR, Williams LR, Tolbert MA (1995) In: Barker JR (ed) *Advanced series in physical chemistry*, vol.3. Progress and problems in atmospheric chemistry. World Scientific, Singapore, p771
- Molina MJ, Molina LT, Golden DM (1996) *J Phys Chem* 100: 12888
- Robinson GN, Worsnop DR, Jayne JT, Kolb CE, Davidovits P (1997) *J Geophys Res* 102: 3583
- (a) Hanson DR, Ravishankara AR (1992) *J Geophys Res* 96: 323; (b) Hanson DR, Ravishankara AR, Solomon S (1994) *J Geophys Res* 99: 3615
- (a) Tolbert MA (1994) *Science* 264: 527 (b) Tolbert MA (1996) *Science* 272: 1597
- Seinfeld JH, Pandis SN (1998) *Atmospheric chemistry and physics. From air pollution to climate change*. Wiley-Interscience, New York
- Abbatt JPD, Nowack JB (1997) *J Phys Chem A* 101: 2131
- Waschewsky GCG, Abbatt JPD (1999) *J Phys Chem A* 103: 5312
- (a) Carslaw KS, Peter Th, Clegg SL (1997) *Rev Geophysics* 35: 125; (b) Tabazadeh A, Toon OB, Clegg SL, Hamill P (1997) *Geophys Res Lett* 24: 1931
- Phillips LF (1994) *Aust J Chem* 47: 91
- Klassen JK, Nathanson GM (1996) *Science* 273: 333
- Fairbrother DH, Johnston H, Somorjai G (1996) *J Phys Chem* 100: 13696
- Radüge C, Pflumio V, Shen YR (1997) *Chem Phys Lett* 274: 140
- (a) Baldelli S, Schnitzer C, Shultz MJ, Campbell DJ (1997) *J Phys Chem B* 101: 10435; (b) Schnitzer C, Baldelli S, Shultz MJ (1999) *Chem Phys Lett* 313: 416
- Duncan L, Schindler LR, Roberts JT (1999) *J Phys Chem B* 103: 7247
- Morris JR, Behr PM, Antman MD, Ringeisen BR, Splan J, Nathanson GM (2000) *J Phys Chem A* 104: 6738
- Kusaka I, Wang ZG, Seinfeld JH (1998) *J Chem Phys* 108: 6829
- Morita A, Hynes JT (to be submitted)
- Hofmannsievart R, Castleman AW (1984) *J Phys Chem* 88: 3329
- Akhmatskaya EV, Apps CJ, Hillier IH, Masters AJ, Watt NE, Whitehead JC (1997) *Chem Commun* (7): 707
- Arstila H, Laasonen K, Laaksonen A (1998) *J Chem Phys* 108: 1031
- Re S, Osamura Y, Morokuma K (1999) *J Phys Chem A* 103: 3535
- Larson LJ, Kuno M, Tao FM, (2000) *J Chem Phys* 112: 8830
- Al-Halabi A, Bianco R, Hynes JT (2002) *J Phys Chem A* 106: 7639
- Kathmann SM, Hale BN (2001) *J Phys Chem B* 105: 11719
- Atkins PW (1994) *Physical chemistry*, 5th ed. Freeman, New York, p C18, Table 9.1
- (a) Devlin JP, Buch V (1995) *J Phys Chem* 99: 16534; (b) Devlin JP, Buch V (1997) *J Phys Chem B* 101: 6095
- (a) Ando K, Hynes JT (1995) *J Mol Liq* 64: 25; (b) Ando K, Hynes JT (1997) *J Phys Chem* 101: 10464; (c) Devlin JP, Uras N, Sadlej J, Buch V (2002) *Nature* 417: 269
- Gertner BJ, Hynes JT (1996) *Science* 271: 1563
- Schmidt MW, Baldrige KK, Boatz JA, Elbert ST, Gordon MS, Jensen JJ, Koseki S, Matsunaga N, Nguyen KA, Su S, Windus TL, Dupuis M, Montgomery JA (1993) *J Comput Chem* 14: 1347

32. Stevens WJ, Bash H, Krauss M (1984) *J Chem Phys* 81: 6026
33. Hariharan PC, Pople JA (1973) *Theor Chim Acta* 28: 213
34. Pietro WJ, Francl MM, Hehre WJ, DeFrees DJ, Pople JA, Binkley JS (1982) *J Am Chem Soc* 104: 5039
35. Spitznagel GW (1982) Diploma. Erlangen
36. Clark T, Chandrasekhar J, Spitznagel GW, Schleyer P (1983) *J Comput Chem* 4: 294
37. (a) Day PN, Jensen JH, Gordon MS, Webb SP, Stevens WJ, Krauss M, Garmer D, Basch H, Cohen D (1996) *J Chem Phys* 105: 1968; (b) Chen W, Gordon MS (1996) *J Chem Phys* 105: 11081
38. Hayward JA, Reimers JR (1997) *J Chem Phys* 106: 1518
39. Ishida K, Morokuma K, Komornicki A (1977) *J Chem Phys* 66: 2153, and references therein
40. Kiefer PM, Hynes JT (2002) *J Phys Chem A* 106: 1850
41. Gertner BJ, Hynes JT (1998) *Faraday Discuss* 110: 301
42. Morokuma K, Muguruma C (1994) *J Am Chem Soc* 116: 10316
43. Re S, Osamura Y, Suzuki Y, Schaefer HF (1998) *J Chem Phys* 109: 973
44. Haynes DR, Tro NJ, George SM (1992) *J Phys Chem* 96: 8502
45. Hanson DR (1998) *J Phys Chem A* 102: 4794
46. Bianco R, Hynes JT (1999) *J Phys Chem A* 103: 3797